Isothermal Crystallization Kinetics of Chain-Extended PET

L. SORRENTINO,[1] S. IANNACE,[2] E. DI MAIO,[1] D. ACIERNO[1]

[1]Department of Materials and Production Engineering, University of Naples, ''Federico II,'' Naples, Italy

[2]Institute of Composite and Biomedical Materials, CNR, P.le Tecchio 80, 80125 Naples, Italy

Received 16 June 2003; revised 28 February 2005; accepted 16 March 2005
DOI: 10.1002/polb.20480
Published online in Wiley InterScience (www.interscience.wiley.com).

ABSTRACT: The crystallization behavior of a commercial chain-extended PET (foam grade) was evaluated and compared to that of bottle-grade PET. Cold and melt isothermal crystallization were analyzed by using the Avrami model. The foam grade PET showed a slower crystallization kinetic compared to the bottle-grade PET. The Hoffman-Lauritzen analysis showed that the energetic barriers to nucleation and molecular mobility were higher for the chain-extended PET. This resulted in a lower nucleation rate in both cold and melt crystallization. ©2005 Wiley Periodicals, Inc. J Polym Sci Part B: Polym Phys 43: 1966–1972, 2005
Keywords: isothermal crystallization kinetics; barrier energy; branching

INTRODUCTION

The polymer crystallization phenomena are very important from different points of view. The molecules dimensions prevent the complete packing of chains, leaving a variable amount of amorphous phase. The presence of crystalline phase leads to materials with enhanced mechanical and gas barrier properties. Amorphous polymers are needed in those applications where it is necessary to ensure the absence of crystals for the postprocessing of intermediate manufacts (e.g., blow molding and thermoforming). It is therefore of great importance to know the crystallization kinetics to optimize the different steps of the overall process. In particular, the thermoforming process of PET is performed on amorphous sheets at temperature above T_g and close to the crystallization temperature of the materials. The optimization of the entire process can be achieved by using appropriate models able to predict the evolution of crystallinity as a function of the thermal history and temperature profile in the sheets. Another application that requires the knowledge of the crystallization kinetics of PET is foaming. In this case, chain-extended PET are utilized because one of the critical properties for foamibility is the presence of strain hardening elongational viscosity, which can be obtained by increasing the molecular weight (MW) and molecular weight distribution (MWD) of the polymer or by using branched macromolecules.[1–3]

The crystallization kinetics of linear PET (both isothermal[4,5] and nonisothermal[6–8]) has been widely studied. The Avrami equation is the first (empirical) equation used to accomplish the crystallization growth. It correlates the volumetric fraction of crystalline phase $\alpha_v^c(t)$ in function of time in an isothermal process:[9–11]

$$\alpha_v^c(t) = 1 - \exp(-kt^n) \tag{1}$$

where k is the kinetic constant, function of nucleation and growth rates, and n is the Avrami exponent, an integer from 0 to 4, which is the sum of two terms: one takes into account the nucleation type (homogeneous or heterogeneous, 1 or 0, respectively) and another the number of crystal growth directions (one-, bi-, or

Correspondence to: L. Sorrentino (E-mail: lsorrent@unina.it)

Journal of Polymer Science: Part B: Polymer Physics, Vol. 43, 1966–1972 (2005)

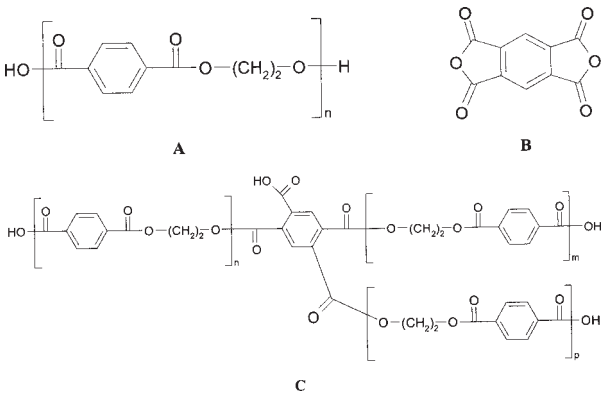

Figure 1. Structures of PET (A), PMDA (B). and a branched structure obtained by their reaction.

three-dimensional growth, from 1 to 3). This equation is in good agreement with isothermal crystallization data only for short times (depending by the crystallization temperature), due to some model simplifications such as constant polymeric phase density, constant nuclei density and crystal shape, constant radial growth rate, or no secondary crystallization. However, in addition to primary aggregation processes as in LDPE,[12,13] secondary crystallization occurs in PET[14–16] as well as in other common and engineering polymers.[17–22]

For some time many efforts have been made to exceed these limits, taking into account the incomplete crystallization,[23,24] the different phase density of amorphous and crystalline phases,[25,26] variations of crystal growth rate,[27] the two different nucleation mechanisms,[28] and the contact of the spherulities.[29,30]

The equation obtained by this corrections is formerly similar to eq 1, but the terms have a different meaning:

$$X_c(t) = 1 - \exp[-k(t - t_0)^n] \qquad (2)$$

where $X_c(t)$ is the relative crystallinity, that is, the ratio between crystal fraction at time t and final crystal fraction, k is the kinetic constant, n is the Avrami constant, now not an integer, and t_0 is the induction time, that is, the time between the stabilization of the temperature and the time at which the crystallization starts.

In this work, the crystallization behavior of a commercial chain-extended PET with high molecular (foam grade) weight was experimentally evaluated and modeled by using the Avrami model (eq. 2). The cold and melt isothermal crystallization were analyzed by using the theory of Hoffman-Lauritzen, which allowed the determination of the main thermodynamic properties involved in the nucleation and growth mechanism of the crystals.[31] The results were compared to those relative to the crystallization phenomena occurring in bottle grade PET, which were taken from Lu et al.[4]

MATERIALS AND METHODS

The commercial chain extended PET (MPET) with an intrinsic viscosity of 1.25 dL/g was kindly supplied by Mossi & Ghisolfi S.p.A. The reported molecular weight distribution was characterized by a $M_w = 160{,}000$ with high polydispersity ($M_n = 22{,}000$).

Dynamic DSC scans were performed on dried samples (110 °C for 12 h in a vacuum oven) to identify the temperature ranges for isothermal tests. The samples were heated from 25 to 290 °C at 10 °C/min (I scan) and then taken at 290 °C for 4 min to cancel previous thermal history effects. The materials were then cooled to 25 °C at 10 °C/min (II scan) and then reheated again to 290 °C at 10 °C/min (III scan).

Before all the isothermal cold crystallization tests, PET samples were first melted at 290 °C for 4 min in the DSC cell to clear the previous thermal history, and then quenched in liquid nitrogen to avoid crystal nucleation. The samples were kept in anydrous conditions before the isothermal test. For all melt crystallization experiments the samples were melted at 290 °C for 4 min and then quickly cooled at 40 °C in the DSC cell to the test temperature.

All the tests were performed in a purge flow of nitrogen to avoid the hydrolysis effects of oxygen by using a TA Instruments DSC 2920.

RESULTS AND DISCUSSION

PET molecular structure is represented in Figure 1(A). Chain extension agents are used to enhance the molecular weight, linking end groups of two macromolecular chains. The chain extender used to produce the analyzed polymer is pyromellitic dianhydride, PMDA [Fig. 1(B)], that reacts with the hydroxylic end group of two different PET macromolecules and forms two carboxylic groups. But at high temperatures these carboxylic groups can react with —OH

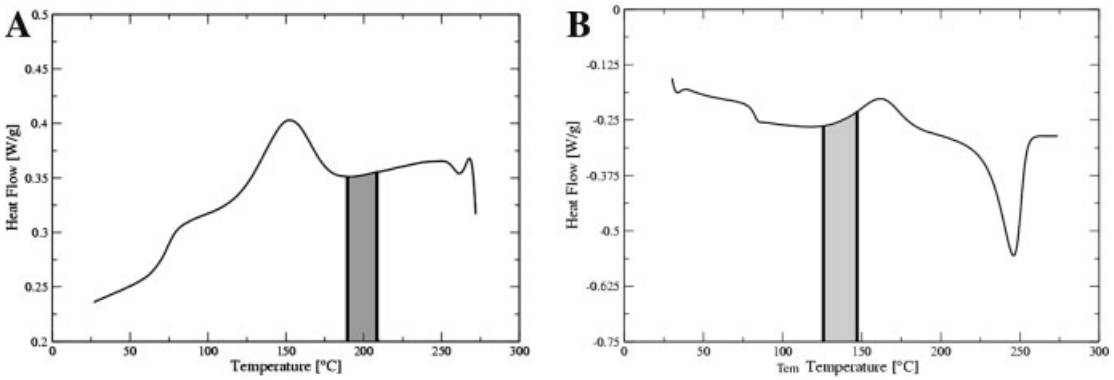

Figure 2. DSC thermograms during II scan (A) and III scan (B) at 10 °C/min.

groups leading to a branched structure and producing one H_2O molecule, as in Figure 1(C).[32–35]

The cooling (II scan) and heating (III scan) DSC curves of chain extended PET are reported in Figure 2. As shown in Figure 2(A), MPET crystallized during the cooling scan with an exothermal peak ranging from 205 to 125 °C. The isothermal melt crystallization kinetics were investigated at temperatures ranging from 190 to 209 °C [gray area in Fig. 2(A)]. As shown in Figure 2(B), the crystallization was not complete and further crystallization occurred during the subsequent heating scan. The isothermal cold crystallization was evaluated at temperatures ranging from 125 and 145 °C [gray area in the Fig. 2(B)]. Both ranges were chosen to assure that the heat flow and the evolution of relative crystallinity could be slow enough to be precisely measured, as verified by curves in Figures 3 and 4 for the cold crystallization and Figures 5 and 6 for the melt crystallization.

Using the heat flow data, the relative crystallinity was evaluated using eq 3:

$$X_{C,rel}(t) = \Delta H(t)/\Delta H_{\mathrm{TOT}} \tag{3}$$

where $\Delta H(t)$ is the heat of crystallization at time t, and ΔH_{TOT} is the total heat of crystallization. In the cold crystallization temperature range, the high undercooling of polymer melt leads to a high nucleation rate, but the overall crystallization process is hindered by the low chain folding mobility. The increase of temperature leads to a faster crystallization rate (Figs. 3 and 4) due to the increase of macromolecular mobility. As expected, an opposite behavior was observed in the melt crystallization temperature range (Fig. 5 and 6). At a temperature near the melting temperature, the molecular mobility is very high, but the limiting phenomenon is now the low nucleation rate because of the low undercooling. In this case, an increase of temperature

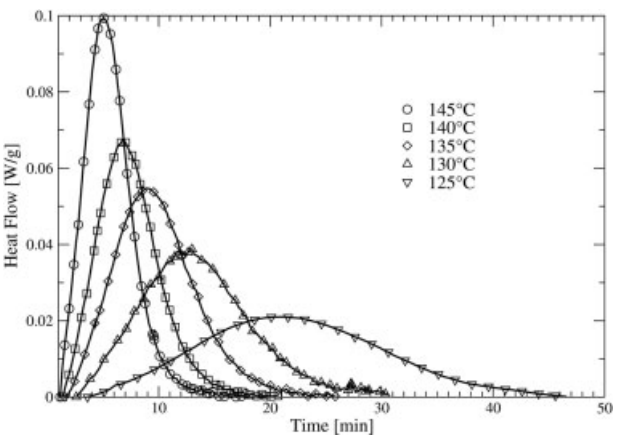

Figure 3. Heat flows versus time of low-temperature isotherms, between 125 and 145 °C.

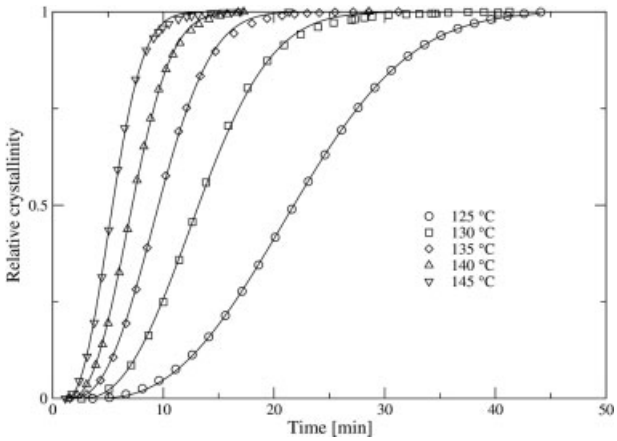

Figure 4. Relative crystallinity curve of low-temperature isotherms, between 125 and 145 °C.

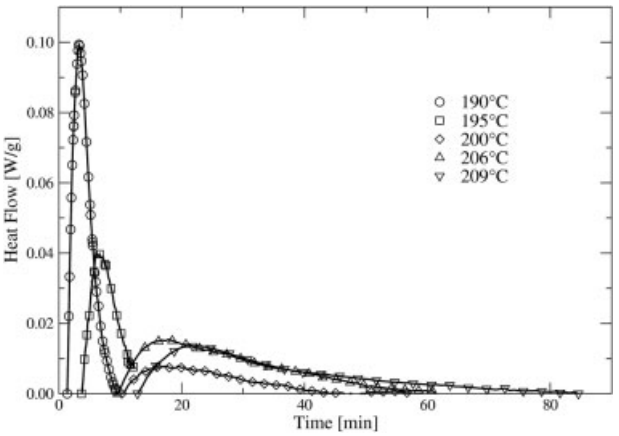

Figure 5. Heat flows versus time of high-temperature isotherms, between 190 and 209 °C.

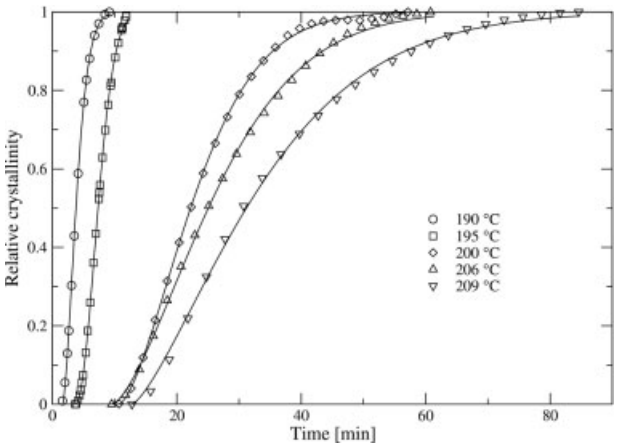

Figure 6. Relative crystallinity curve of high-temperature isotherms, between 190 and 209 °C.

lowers the overall crystallization rate and the polymer crystallization takes place at longer times.

A good agreement between the Avrami model (eq. 2) and the experimental data was observed, as shown in Figures 3–6. The good fitting is an indirect evidence that secondary crystallization is negligible and, as described below, the Avrami parameters can be used to analyze the crystallization mechanism of the high molecular weight PET studied in this work.

As listed in Table 1, the Avrami exponent n, which represents the nucleation mechanism and the number of growth directions, is nearly 3. Most of the data varied from a maximum of 3.2 to a minimum of 2.8 except for one testing condition (206 °C) where n was 2.2. These results are sligthly higher than those reported by Lu et al.,[4] as listed in Table 2, suggesting that the nucleation and growth mechanisms were slightly influenced by the modification of the macromolecular structure induced by the chain extension/branching reaction.

The induction time decreased with temperature in the cold crystallization range, due to the raising of the molecular mobility. On the contrary, in melt crystallization temperature range the induction time grows because of the difficulty to nucleate a high number of stable nuclei. The low undercooling induces a weak thermodynamical instability and increases the critical radius of the nucleus. For this reason, according to experimental data, in the cold crystallization range t_0 is less sensitive to temperature respect to the melt crystallization range.

To compare the crystallization rates of MPET with the bottle grade PET from ref.[4], the crystallization half-time $t_{1/2}$ (the time at which the relative crystallinity reaches the 50%), instead of the crystal growth rate G according to ref.[36], was used to evaluate the Hoffman-Lauritzen thermodynamical parameters U and K_g (eq 4):

$$t_{1/2}^{-1}=t_{1/2,0}^{-1}\exp[-U/R(T-T_C)]\exp[-K_g/fT_C\Delta T], \quad (4)$$

where $t_{1/2,0}$ is a preexponential factor, T_C is the crystallization temperature, ΔT (melt undercooling) is the difference between the thermodynamic melt temperature T_m^0 and the actual temperature T, f is a corrective factor equal to $2T_C/(T_C+T_m^0)$. The U parameter is the heat of activa-

Table 1. Values of Avrami Model Parameters Chain-Extended PET (MPET)

Parameter	Cold Crystallization					Melt Crystallization				
Temperature (°C)	125	130	135	140	145	190	195	200	206	209
t_0 (min)	3.6	2.6	1.6	1.4	1.2	1.6	3.8	10.7	9.5	12.8
n	2.8	2.8	3.0	3.2	3.0	2.9	2.8	2.9	2.2	3.1
K * 10^3 (min^{-n})	0.12	0.46	0.77	1.10	4.00	12.00	1.90	0.12	0.049	0.029
$t_{1/2}$ (min)	22.1	13.2	9.55	7.3	5.4	3.75	7.2	21	25	28

Table 2. Values of Avrami Model Parameters, Bottle Grade PET (from ref. 4)

Parameter	Cold Crystallization						Melt Crystallization					
Temperature (°C)	117.9	119.8	121.7	123.6	125.5	127.5	211.8	213.7	215.7	217.6	219.5	221.4
n	2.6	2.5	2.6	2.7	2.6	2.5	2.7	2.7	2.7	2.5	2.5	2.4
K * 10^3 (min^{-n})	1.24	2.66	5.19	7.24	18.60	68.00	12.60	7.99	4.75	4.20	3.49	2.71
$t_{1/2}$ (min)	11.4	9.26	6.57	5.42	4.25	3.45	4.41	5.22	6.33	7.71	8.72	10.1

tion of the chain diffusion, while the K_g parameter is related to the free energy of formation of a nucleus of critical size.

In Figure 7 the experimental data (square marks) and the fitting values of $1/t_{1/2}$ (solid line) versus crystallization temperature are compared to those of bottle grade PET, taken from Lu et al.[4]

The curve of the chain-extended PET exhibited a peak value that was one-third of the bottle-grade PET, confirming the lower crystallization rate of the MPET at every temperature. The energetic term U, related to the molecular mobility, was evaluated from the experimental data obtained at lower temperatures (T = 125–145 °C) while the nucleation term K_g from the data at higher temperatures (T = 190–209 °C). As reported in Table 3, the curve of the MPET is characterized by higher values of U and K_g.

The value of U shows that the diffusional motions of chains from the amorphous phase to the growing nuclei (crystalline phase) are reduced by the increased MW, MWD, and eventual presence of branched macromolecules, as also reported in ref.[37] The rheological behavior of chain-extended and bottle-grade PET are compared in Figure 8. The complex viscosity of the MPET is higher in the whole frequency range and does not display the typical Newtonian behavior at low frequency, as observed in bottle-grade PET. This behavior can be related not only to an increase of molecular weight of PET but also to the presence of irregularities along the macromolecules that modify the dependence of complex viscosity η^* with frequency.[39–41] The modification of rheological properties is, in fact, associated to the increase in average relaxation time and broadening of relaxation time distribution as a result of chain extension and branching, as already reported by Xanthos et al.[1–3]

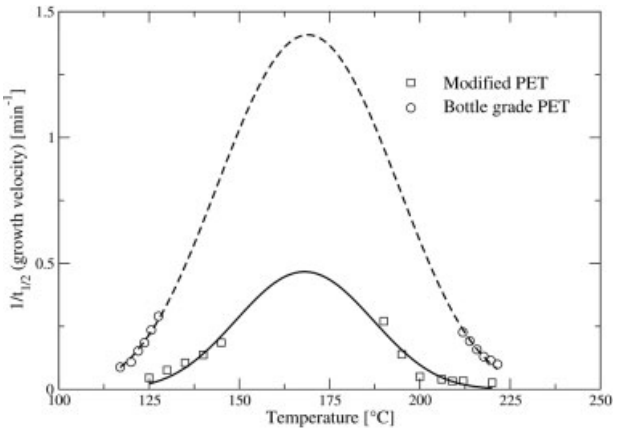

Figure 7. Crystallization rate curves of modified (solid line) and bottle-grade (dashed line) PET.

The theoretical expression of K_g can be used to make some considerations about the effect of modification of the polymer on the structural characteristics of crystals (eq. 5).

$$K_g = (4b\sigma\sigma_e T_m^0)/(\Delta H_f^0 k) \quad (5)$$

The slight increase of K_g observed in MPET can be due to several factors related to the thermodynamic properties of the crystals. The equilibrium melting point T_m^0 of MPET was evaluated by using the well known Hoffman-Weeks[42] analysis and reported in Figure 9. The melting point of the MPET (T_m^0 = 271 °C) was found to be significantly lower than that of bottle grade PET[4] (T_m^0 = 290°C). For this reason, the slight increase of K_g can be attributed to the increase of the free surface energies σ and σ_e (respectively, the energy of the chain folding side and of its end) probably caused by the presence of some structural irregularities along the MPET macromolecule.

X-ray analysis showed that the crystal morphology of the MPET and bottle-grade PET were characterized by the same diffraction peaks (Fig. 10), suggesting that the chemical modification did not affect the packing distance in crystals.

Table 3. Energetic Barrier Values

Polymer Type	U J mol^{-1}	K_g °C^2
Chain extended PET	8′589	4.75 10^5
Bottle grade PET	5′669	4.39 10^5

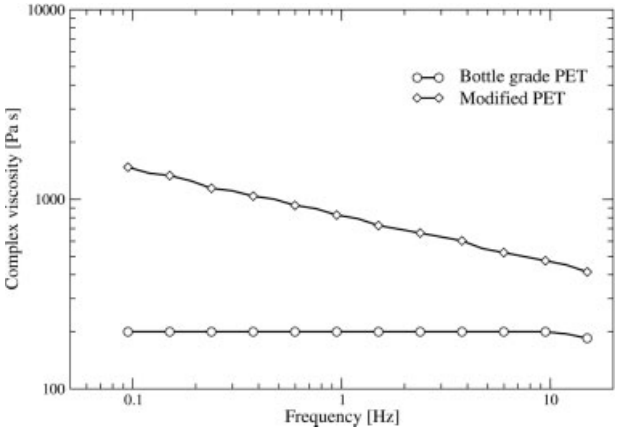

Figure 8. Rheological behavior of different types of PET.

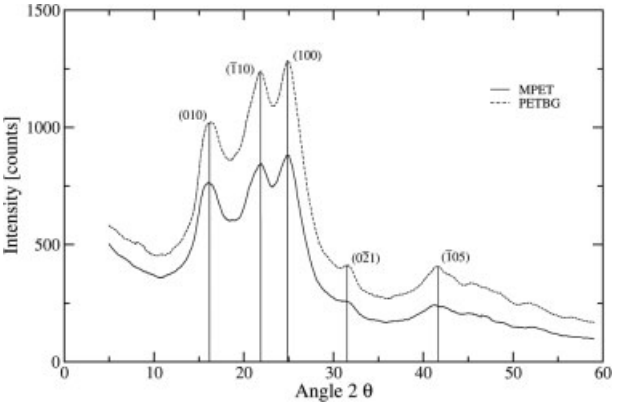

Figure 10. X-ray pattern of bottle-grade PET (PETBG) and chain-extended PET (MPET).

The heat of fusion ΔH_f is therefore expected to be the same in both MPET and bottle-grade PET.

These variations can be justified if branching occurred during chemical modifications with PMDA, that, influencing the perfection degree of crystals leads to crystalline phase structure alterations. In this way the growing nucleus, to form a stable aggregate, meets a higher energy barrier to overcome in the chain extended PET respect to that of the standard polymer.

The effect of broadening of the molecular weight on crystallization of foaming grade PET has not been studied in detail so far; therefore, it is difficult to establish clear correlations between the MWD and the crystallization behavior of the PET studied in this work. On the contrary, the effect of polydispersity on crystallization kinetics was recently investigated on HDPE.[43] The authors found that the isothermal crystallization behavior of materials with broad MWD followed same trends as crystallization of materials with narrow MWD, even if some small differences caused by the broad MWD were observed. Due to the lack of literature data on PET more work on this issue should be done to clarify the role of the MWD versus branching on the crystallization behavior of these foaming-grade PET.

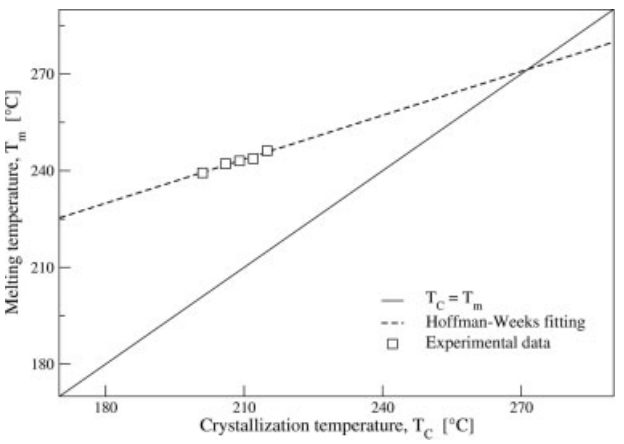

Figure 9. Hoffman-Weeks regression of chain-extended PET data for T_{m0} evaluation.

CONCLUSIONS

The crystallization behavior of a commercial chain-extended PET with high molecular weight was evaluated and compared to that of bottle-grade PET. The commercial chain-extended PET showed slower crystallization kinetics in the temperature ranges analyzed. The energetic barriers to nucleation (K_g) and molecular mobility (U) of the chain foldings moving from the melt to the growing crystals were higher for the chain-extended PET, suggesting that the chain-extending reactions introduced some variations in the macromolecular structure, probably due to partial branching, as also suggested by other authors.[1–3,32–35] This resulted in a lower nucleation rate in both cold and melt crystallization. More work should be done to clarify the role of the MWD versus branching on the crystallization behavior of foaming grade PET.

REFERENCES AND NOTES

1. Dhavalikar, R.; Yamaguchi, M.; Xanthos, M. J Polym Sci Part A: Polym Chem 2003, 41, 958–969.
2. Xanthos, M.; Yilmazer, U.; Dey, S. K.; Quintans, J. Polym Eng Sci 2000, 40, 554–566.

3. Xanthos, M.; Wan, C.; Dhavalikar, R.; Karayannidis, G. P.; Bikiaris, D. N. Polym Int 2004, 53, 1161–1168.
4. Lu, X. F.; Hay, J. N. Polymer 2001, 42, 9423–9431.
5. Wang, Z. G.; Hsiao, B. S.; Sauer, B. B.; Kampert, W. G. Polymer 1999, 40, 4615–4627.
6. Piccarolo, S.; Brucato, V.; Kiefle, Z. Polym Eng Sci 2000, 40, 1263–1272.
7. Ozawa, T. Polymer 1971, 12, 150–157.
8. Sajkiewicz, P.; Carpaneto, L.; Wasiak, A. Polymer 2001, 42, 5365–5370.
9. Avrami, M. J Chem Phys 1939, 7, 1103–1112.
10. Avrami, M. J Chem Phys 1940, 8, 212–224.
11. Avrami, M. J Chem Phys 1941, 9, 177–184.
12. Maderek, E.; Strobl, G. R. Colloid Polym Sci 1983, 261, 471–476.
13. Strobl, G. R.; Engelke, T.; Maderek, E.; Urban, G. Polymer 1983, 24, 1585–1589.
14. Sauer, B. B.; Kampert, W. G.; Neal Blanchard, E.; Threefoot, S. A.; Hsiao, B. S. Polymer 2000, 41, 1099–1108.
15. Elsner, G.; Koch, M. H. J.; Bordas, J.; Zachmann, H. G. Makromol Chem 1981, 182, 1263–1269.
16. Santa-Cruz, C.; Stribeck, N.; Zachmann, H. G.; Balta-Calleja, F. J. Macromolecules 1991, 24, 5980–5990.
17. Verma, R. K.; Hsiao, B. S. Trends Polym Sci 1996, 9, 312–319.
18. Bassett, D. C.; Olley, R. H.; Al Raheil, I. A. M. Polymer 1988, 29, 1745–1754.
19. Hsiao, B. S.; Gardner, K. H.; Wu, D. Q.; Chu, B. Polymer 1993, 34, 3986–3995.
20. Lattimer, M. P.; Hobbs, J. K.; Hill, M. J.; Barham, P. J. Polymer 1992, 33, 3971–3973.
21. Verma, R. K.; Marand, H.; Hsiao, B. S. Macromolecules 1996, 29, 7767–7775.
22. Verma, R. K.; Kander, R. G.; Velikov, V.; Marand, H.; Chu, B.; Hsiao, B. S. Polymer 1996, 37, 5357–5365.
23. Wunderlich, B. Macromolecular Physics: Crystal Nucleation, Growth, Annealing; Academic Press: London, 1976; vol. 2.
24. Lin, C. C. Polym Eng Sci 1983, 23, 113–116.
25. Price, F. P. In Wunderlich, B., Ed.; Macromolecular Physics: Crystal Nucleation, Growth, Annealing; Academic Press: London, 1976; vol. 2.
26. Mandelkern, L.Crystallization of Polymers; Cambridge University Press: Cambridge, 1964; vol. 2.
27. Kim, S. P.; Kim, S. C. Polym Eng Sci 1991, 31, 110–115.
28. Banks, W.; Sharples, A. J Polym Sci Part A: Gen Papers 1964, 2, 4059–4067.
29. Tobin, M. C. J Polym Sci: Polym Phys 1974, 12, 399–406.
30. Tobin, M. C. J Polym Sci: Polym Phys 1976, 14, 2253–2257.
31. Hoffman, J. D.; Lauritzen, J. I., Jr. J Res Natl Bour Stand A: Phys Chem 1961, 65A, 297–336.
32. Khemani, K. C. Annual Technical Conference, 56th ed.; Soc Plastics Eng 1998, 2, 1934–1938.
33. Chae, H. G.; Kim, B. C.; Im, S. S.; Han, Y. K. Polym Eng Sci 2001, 41, 1133–1139.
34. Rhein, R. A.; Ingham, J. D. Polymer 1973, 14, 466–468.
35. Bratychak, M.; Brostow, W.; Castano, V. M.; Donchak, V.; Gargai, H. Mater Res Innovat 2002, 6, 153–159.
36. Chan, T. W.; Isayev, A. I. Polym Eng Sci 1994, 34, 461–471.
37. Jayakannan, M.; Ramakrishnan, S. J Appl Polym Sci 1998, 74, 59–66.
38. Incarnato, L.; Scarfato, P.; Di Maio, L.; Acierno, D. Polymer 2000, 41, 6825–6831.
39. Wang, X. S.; Yan, D.; Tian, G. H.; Li, X. G. Polym Eng Sci 2001, 41, 1655–1664.
40. Rosu, R. F.; Shanks, R. A.; Bhattacharya, S. N. Polym Int 2000, 49, 203–208.
41. Lohse, D. J.; Milner, S. T.; Fetters, L. J.; Xenidou, M.; Hadjichristidis, N.; Mendelson, R. A.; Garcia-Franco, C. A.; Lyon, M. K. Macromolecules 2002, 35, 3066–3075.
42. Hoffman, J. D.; Weeks, J. J Res Natl Bour Stand A: Phys Chem 1962, 66A, 13–28.
43. Krumme, A.; Lehtinen, A.; Viikna, A. Eur Polym J 2004, 40, 359–369.